

# Analysis and Application of a Hybrid Motor Structure Convenient to Modify the Magnet and Reluctance Torques on the Rotor

Esra Kandemir Beser<sup>†</sup>, Sabri Camur\*, Birol Arifoglu\* and Ersoy Beser\*

**Abstract** – This paper presents a hybrid motor prototype convenient to modify the magnet and reluctance torques. The rotor of the prototype consists of magnet and reluctance parts, so the generated torque includes both magnet and reluctance torques. A considerable feature of the motor is that the ratio of the magnet and reluctance parts can be modified on the rotor and the rotor hybridization ratio can be varied. Another important point is the mechanical angle between the parts changed by means of the suitable construction of the parts on the rotor shaft. Finite element (FE) analysis was carried out for the proposed motor and static torque measurements were realized. The FE results were compared with the experimental results. Average torque and maximum torque values were obtained and three dimensional 3-D graphs were formed by using the experimental data. It is possible to make different combinations by changing the parts and the angle between the parts due to the proposed motor. So the magnet and reluctance torques are modified and different combinations give different torque behavior.

**Keywords:** Hybrid motor, Permanent magnet, Reluctance, Axially laminated, Hybridization

## 1. Introduction

Parallel to the growing technology, the demand for electrical motors with different characteristics has been gradually increasing in the industry. Therefore, the research concerning improvement of the electrical motors has been widely studied in the literature. New motor types have been proposed and existing motor types have been developed in these studies.

Magnet type motors and reluctance motors are among the popular subjects for the electrical motors in the literature. Various structures have been discussed and realized for these motors. Particularly, the interest in magnet type motors has been increased along with the improvements in the features of the magnet materials. The applications of the magnet type motors can be classified as permanent magnet synchronous motors (PMSM) and brushless dc motors (BLDC). Although performance of the magnet type motors is perfect at base speed, their speed range is quite narrow [1, 2].

Reluctance motors include no magnet material on their rotors. This feature removes the demagnetization risk and makes the motor suitable for high temperatures. Reluctance motors operate according to the reluctance principle. They can be separated into two groups as switched reluctance motors (SRM) and synchronous reluctance motors (SynRM). SRM has salient pole stator and rotor structure. The stator pole and rotor pole numbers are designed as different from each other. Salient pole, axially or

transversally laminated rotor type can be preferred for SynRM. High saliency ratio is obtained for axially and transversally laminated rotors. However, saturation effects occur at high current values [1, 2].

Permanent magnet assisted reluctance motors (PMA-SynRM) have been designed to combine the advantages of magnet type and reluctance motors. Since these motors have high power density, high power factor, high efficiency and wide speed range, they become a considerable and popular topic [3, 4]. Because the produced torque is a combination of magnet and reluctance torques, this motor type can be called as a hybrid motor. The rotor can be designed in many different structures to provide both magnet and reluctance torques [1-11].

Related to the interest for the permanent magnet assisted reluctance motors, analysis and application of a hybrid motor structure is presented in this paper. The proposed motor consists of two components as magnet and reluctance parts. The motor offers the ability for modifying the hybridization ratio of these parts on the rotor. Another significant feature is the ability to rotate the parts with respect to one another. In the following section the proposed hybrid motor is described in detail. FE analysis is presented in Section 3. Static torque measurements are explained in Section 4 and considerable results are given and discussed in Section 5. Finally, the results of the complete paper are presented in Section 6.

## 2. Proposed Hybrid Motor

The proposed hybrid motor consists of two separate structures as magnet and reluctance parts. Magnet and

<sup>†</sup> Corresponding Author: Dept. of Electrical Engineering, Kocaeli University, Turkey. (esrakandemir@kocaeli.edu.tr)

\* Dept. of Electrical Engineering, Kocaeli University, Turkey. (scamur@kocaeli.edu.tr, barif@kocaeli.edu.tr, ebeser@kocaeli.edu.tr)

Received: January 24, 2011; Accepted: February 9, 2012

reluctance parts are combined on the rotor and then a hybrid motor configuration is formed. These parts can be arranged along the stator, thus the hybridization ratio on the rotor can be varied [11]. Magnet and reluctance parts will be explained in the following.

### 2.1 Magnet part

Magnet part consists of 6 pieces. Magnet material was preferred as high-energy NdFeB magnets for this part. Magnets were placed into the rectangular shaped slots. In order to avoid the reduction of the main flux due to magnetic short circuit on the magnets own, air holes were realized between the magnets. A total of 12 magnets are used for each magnet piece and one pole consists of 3 magnets. This part produces magnet torque of the hybrid motor. The Cad drawing and a photograph of the magnet pieces are shown in Fig. 1.

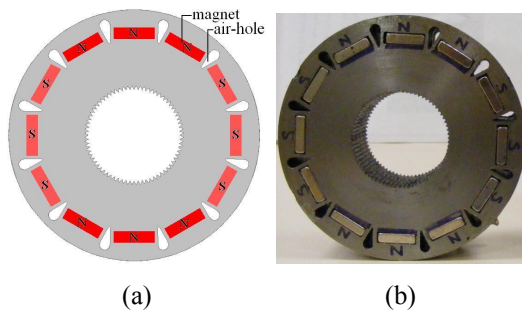


Fig. 1. (a) The Cad drawing; (b) the photograph of the magnet pieces

### 2.2 Reluctance part

Reluctance part was designed as 6 reluctance pieces similar to the magnet part. Axially laminated rotor structure was preferred for the reluctance part to obtain high saliency ratio. In order to generate reluctance torque, magnetic paths are formed in one direction to let the magnetic flux flow and barriers are also formed in one direction to prevent the passing of the magnetic flux in axially laminated rotor structure. Thus, minimum and maximum inductance values are occurred for two positions of the rotor. The ratio between the maximum and the minimum inductance gives the saliency ratio and it directly affects the generated reluctance torque. By using magnetic and non magnetic materials, magnetic paths and barriers were obtained for the axially laminated rotor structure.

The insulation ratio is another considerable point for the reluctance machine and it affects the saliency ratio. The insulation ratio  $W_{ins}$  is defined as

$$W_{ins} = \frac{W_{non}}{W_{non} + W_{mag}} \quad (1)$$

where  $W_{non}$  is the sum of the widths of the non-magnetic material and  $W_{mag}$  is the sum of the widths of the magnetic material [5, 6].

The thickness of both magnetic and non-magnetic material was selected as 1mm. Each reluctance piece has 14 magnetic materials and 13 non-magnetic materials for one pole and then the value of insulation ratio is calculated as 0.48. The insulation ratio is recommended in the range of 0.4-0.6 [5, 6] and 0.33-0.4 [12, 13] to obtain the maximum reluctance torque in different studies in the literature.

Although minimum air-gap length is required for reluctance machines, the air-gap length is limited by the mechanical manufacturing limits. The air-gap length has been achieved as 0.35mm for the reluctance part. This part generates the reluctance torque for the hybrid motor. The Cad drawing and a photograph of the reluctance pieces are shown in Fig. 2.

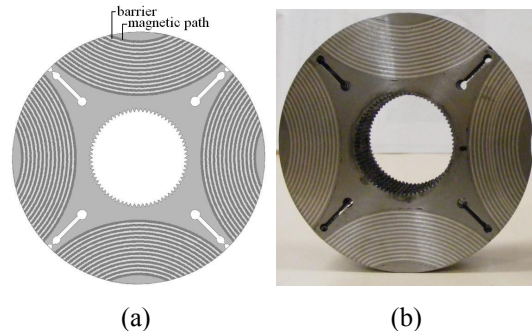


Fig. 2. (a) The Cad drawing; (b) the photograph of the reluctance pieces

### 2.3 Hybrid rotor structure

Magnet and reluctance pieces are arranged on the rotor shaft in various combinations and they form the different rotor hybridization ratios. The stator length allows a maximum of 6 pieces to be arranged. The proposed rotor structure provides to examine seven rotor types as magnet, reluctance and five hybrid structures constituted by magnet and reluctance pieces. Design information of the proposed hybrid motor is given in Table 1.

Another considerable feature of the hybrid rotor is that 5 degree spaced teeth exist on the rotor shaft and also in magnet and reluctance pieces. This feature makes it possible that the pieces can be rotated with respect to each other with 5 mechanical degrees. The principle scheme of the hybrid rotor structure is shown in Fig. 3. It can be seen from Fig. 3 that the mechanical angle between the magnet and reluctance parts is defined as  $\beta$ .

Hybrid rotor structure is formed by arranging the magnet and reluctance pieces in various orders on the rotor shaft. A photograph of the magnet and reluctance pieces and the rotor shaft is given in Fig. 4.

**Table 1.** Design information of the proposed motor

Stator	Rotor (Magnet Part)	Rotor (Reluctance Part)
Outside diameter: 200mm Number of poles: 4 Inner diameter: 125mm Number of slots: 36 Winding: distributed, 8 turns, star Stack length: 240mm Lamination material: M400-50A	Diameter: 123.9mm Magnet material: NdFeB Number of magnets per pole: 3 Rotor material: Steel 1010	Diameter: 124.3mm Magnetic material: Grain oriented M6 Mag. material thickness: 1mm Mag. material per pole: 14 Non-magnetic material: Al Non-mag. material thickness: 1mm Non-mag. material per pole: 13

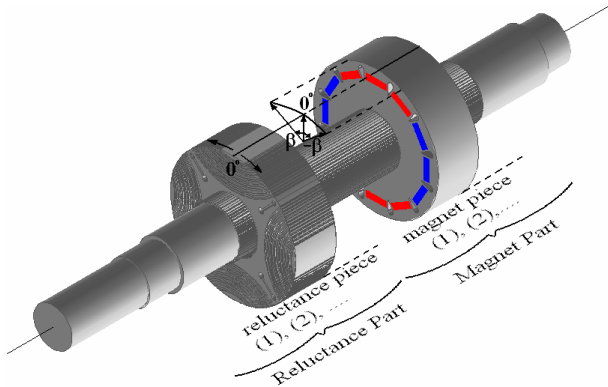


**Fig. 3.** The principle scheme of the hybrid rotor structure



**Fig. 5.** The photograph of the hybrid motor structure for the rotor Hybrid3 at the  $\beta$  value of  $0^\circ$



**Fig. 4.** The photograph of the magnet and reluctance pieces and the rotor shaft

The generated torque is the sum of magnet and reluctance torques in the proposed hybrid motor. The total torque is affected by the ratio of the magnet and reluctance pieces on the rotor. This ratio is defined as the rotor hybridization ratio. Table 2 gives the hybridization ratios and motor names for the proposed motor.

**Table 2.** Hybridization ratios of the proposed motor

Hybridization Ratio	Motor Name
100%Pm	Magnet
83%Pm-17%Reluctance	Hybrid1
67%Pm-33%Reluctance	Hybrid2
50%Pm-50%Reluctance	Hybrid3
33%Pm-67%Reluctance	Hybrid4
17%Pm-83%Reluctance	Hybrid5
100% Reluctance	Reluctance

The magnet and reluctance parts are also rotated with respect to one another by the mechanical angle  $\beta$ . So, the total torque value changes for each situation. In Fig. 5 a photograph of the hybrid motor is given for the rotor Hybrid3 at the  $\beta$  value of  $0^\circ$ .

### 3. Finite Element Analysis

The proposed motor design is first carried out by using two dimensional (2D) finite element method (FEM) by a FE software. As the proposed motor consists of two parts, the geometry of the magnet and reluctance parts are separately formed in the simulation program. Then, the results of the FE analysis is combined for the hybrid motor structures.

The stator of the machine was fed with electrical  $120^\circ$  mode, so only two phases were fed by constant current during the rotor movement of 5 mechanical degrees. The torque profiles related to rotor angle were computed by means of FE method.

Fig. 6 and Fig. 7 show the torque behavior of the Magnet and the Reluctance at the current values of 10A, 20A and 40A, respectively. The reference point is determined as the zero point of the reluctance torque in the analysis.

For the proposed hybrid motor both magnet and reluctance torque exist, and so the total torque ( $T_{hybrid}$ ) can be expressed as

$$T_{hybrid} = a \times T_m + (1-a) \times T_r \quad (2)$$

Here,  $a$  and  $(1-a)$  can be expressed as the magnet and reluctance coefficients,  $T_m$  is the magnet torque and  $T_r$  is the reluctance torque respectively. For this work, since the

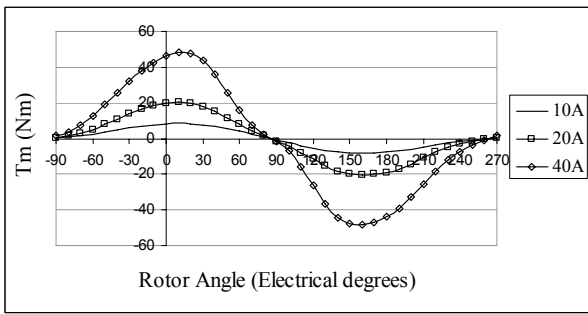


Fig. 6. Torque profile of the Magnet obtained from the FE analysis

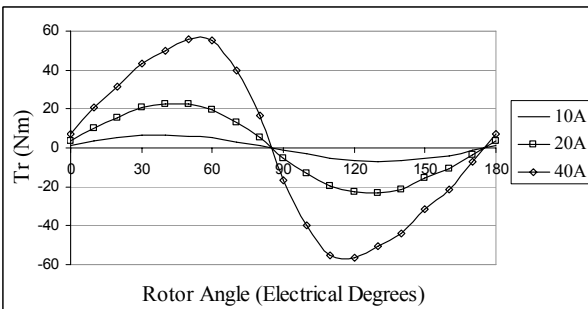


Fig. 7. Torque profile of the Reluctance obtained from the FE analysis

rotor consists of two parts,  $a$  takes the values 0, 1/6, 2/6, ..., 6/6 according to the hybridization of the magnet and reluctance parts. After obtaining the torque profiles of machines the Magnet and the Reluctance, the torque profiles of the hybrid motor structures can be formed considering the Eq. (1).

The torque profiles can also be modified according to the mechanical angle between the magnet and reluctance parts. Consequently, the torque behavior of the hybrid motor structures can be obtained related to the rotor hybridization ratio and the  $\beta$  by using the results of the FE analysis for different current values. The analysis results will be evaluated together with the experimental results in the Section 5.

#### 4. Experimental Study

After completing the FE analysis, the proposed hybrid motor was manufactured and tested on the laboratory type machine test set. The static torque measurements were realized and torque profiles were obtained for the proposed motor.

The machine set consists of a disc brake to lock the rotor and a torque transducer to measure the produced torque. The photograph of the experimental set up is shown in Fig. 8.

The stator winding is fed by a regulated dc source and the rotor is rotated with 5 mechanical degrees. The rotor is

locked by the disc brake and the generated torque is measured by the torque transducer for each rotor position.



Fig. 8. The photograph of the experimental setup

During the static torque measurements, the stator was fed with electrical 120° mode and so only two phases were energized by the constant current value. The rotor hybridization ratio was changed by modifying the combinations of the magnet and reluctance pieces on the rotor. The magnet and reluctance parts were also rotated with respect to each other by 5 mechanical degrees and the mechanical angle  $\beta$  was varied in the range of  $-50^\circ - +15^\circ$ . Therefore 14 different  $\beta$  values were used for 5 hybrid rotor structure and 70 different hybrid rotor types are examined by the static torque measurements.

The torque values were recorded for different current values at each rotor position. The reference point is chosen as the zero point of the reluctance torque during the measurements similar to FE analysis. The results of the static torque measurements are given in the following sections for the rotors having different hybridization ratios.

#### 4.1 Magnet Rotor (the Magnet)

Fig. 9 shows the static torque results of the Magnet at the current values of 10A, 20A and 40A.

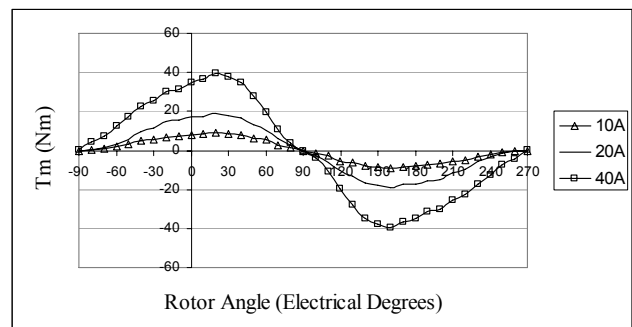
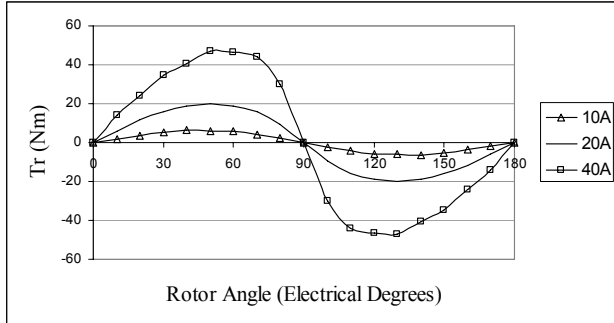


Fig. 9. Measured torque profiles of the Magnet at the current values of 10A, 20A and 40A

### 4.2 Reluctance Rotor (the Reluctance)

The static torque results of the Reluctance are given for the current values of 10A, 20A and 40A in Fig. 10.



**Fig. 10.** Measured torque profiles of the Reluctance at the current values of 10A, 20A and 40A

The output torque for electrical 120° operation mode can also be obtained for the Magnet and the Reluctance by shifting the torque curves. However the static torque measurements were realized for the mechanical angle variation of 5°. So, the points on the torque curves are determined by the steps of 5°. Then the intersection point of the shifted torque curves does usually not correspond with the experimental data. While obtaining the torque profiles for electrical 120° mode, the intersection point of the static torque curves is predicted using the lines constituted by two known points near the intersection point on the curves. The behavior of the output torque of the Magnet and the Reluctance for electrical 120° are given in Fig. 11 at the current value of 20A.

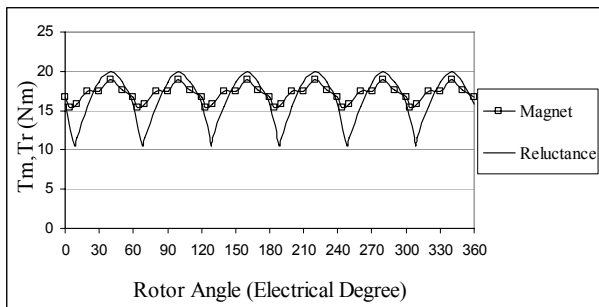


**Fig. 11.** Behavior of the output torque as a function of the rotor angle for electrical 120° mode in the Magnet and the Reluctance referring to the current I=20A

The average torque ( $T_{avg}$ ) and the maximum torque values ( $T_{max}$ ) can be obtained from the torque profiles.  $T_{avg}$  is calculated for electrical 120° operation mode,  $T_{max}$  is calculated to prepare the preliminary study for controlling of the motor. Table 3 reports  $T_{avg}$  and  $T_{max}$  of the Magnet and the Reluctance at different current values.

The method for calculating the average torque can be defined as numerical integrating or trapeze method. The

total area under the torque profile for electrical 120° operation gives the average torque.

**Table 3.** Average torque and maximum torque of the Magnet and the Reluctance

I (A)	Magnet		Reluctance	
	$T_{avg}$ (Nm)	$T_{max}$ (Nm)	$T_{avg}$ (Nm)	$T_{max}$ (Nm)
5	3.55	3.9	1.12	1.4
10	8.02	9	5.05	6.3
20	17.25	18.9	16.55	19.9
30	26.84	29.8	28.68	34.7
40	35.62	39.5	40.06	46.8
50	43.55	47.7	47.14	51.7

### 4.3 Hybrid rotor structures

The hybrid rotor types having different rotor hybridization ratio were examined and the static torque measurements were performed for the hybrid rotors. Since 70 rotor types were obtained for 5 hybrid rotor structure and the measurements were also realized for different current values, so much data occurred. To evaluate the data together 3-D study is required and 3-D graphs were formed by the available data. The average torque and the maximum torque curves related to  $\beta$  and current are shown in Fig. 12 for the 5 hybrid rotor structures.

## 5. Results and Discussion

After completing FE simulations and experimental study, result tables are formed to evaluate the reasonable results. First, calculated results were compared with the experimental results. Since much data occurred due to the different current and  $\beta$  values in the simulations and experiments for the proposed rotor types, it is not suitable to form the tables with all the data. Therefore, the comparison tables were arranged for particular current and  $\beta$  values. Table 4 and Table 5 report the comparison of FE and experimental results of the proposed motor types at different  $\beta$  values referring to the current I=20A for the average torque ( $T_{avg}$ ) and the maximum torque ( $T_{max}$ ), respectively.

It can be seen from Table 4 and Table 5 that the experimental results are similar to the simulation results. The difference between the numerical and experimental results arises from the measurement method. According to the produced torque, some small changes may occur at the rotor position due to the elasticity of the disc brake.

3-D curves in Fig. 12 gives the average torque and the maximum torque values as a function of the variation of  $\beta$  and current for the hybrid rotor structures. To observe the results better 3-D curves were rotated and 2-D curves were obtained for each graph. An example of the rotated 3-D graph is given in Fig. 13 for the  $T_{avg}$  of the Hybrid1.

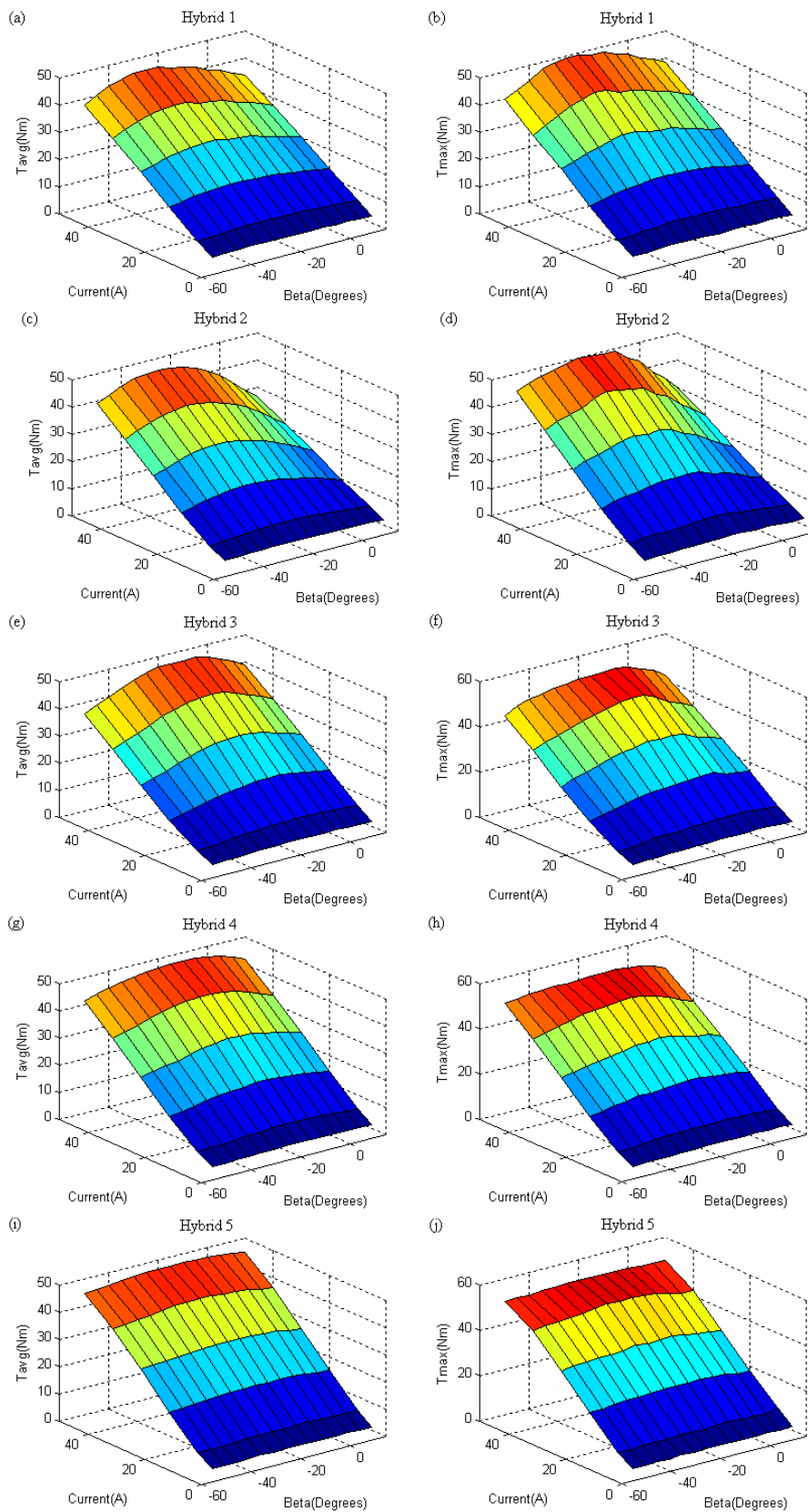


**Fig. 12.** The average torque (a), (c), (e), (g), (i) and the maximum torque curves (b), (d), (f), (h), (j) as a function of  $\beta$  and current for the hybrid rotor structures

**Table 4.** Comparison of FE and experimental results for  $T_{avg}$  at different  $\beta$  values referring to the current  $I=20A$

	$\beta(^{\circ})$	$T_{avg}$ (Nm)													
		Magnet		Hybrid1		Hybrid2		Hybrid3		Hybrid4		Hybrid5		Reluctance	
		Exp	FE	Exp	FE	Exp	FE	Exp	FE	Exp	FE	Exp	FE	Exp	FE
I=20A	15			12.83	14.41	9.80	12.30	13.77	12.69	14.23	14.41	15.14	16.46		
	0	17.25	18.8	15.15	17.32	14.99	16.78	16.28	16.88	16.19	17.37	16.29	18.02	16.55	18.87
	-25			16.63	18.52	16.77	18.44	15.49	18.46	15.98	18.56	16.50	18.69		
	-50			14.11	13.92	12.78	12.32	10.30	13.34	12.77	14.98	14.98	16.80		

**Table 5.** Comparison of FE and experimental results for  $T_{max}$  at different  $\beta$  values referring to the current  $I=20A$

	$\beta(^{\circ})$	$T_{max}$ (Nm)													
		Magnet		Hybrid1		Hybrid2		Hybrid3		Hybrid4		Hybrid5		Reluctance	
		Exp	FE	Exp	FE	Exp	FE	Exp	FE	Exp	FE	Exp	FE	Exp	FE
I=20A	15			14.40	15.69	10.60	13.54	16.00	14.45	16.50	16.66	17.90	19.59		
	0	18.90	20.62	17.40	18.95	15.80	19.03	19.60	19.52	19.10	20.21	19.30	21.43	19.90	22.72
	-25			18.40	20.48	18.60	20.70	17.90	21.14	18.60	21.58	19.40	22.00		
	-50			14.70	14.74	14.30	13.91	11.90	15.41	15.20	17.64	17.80	19.96		

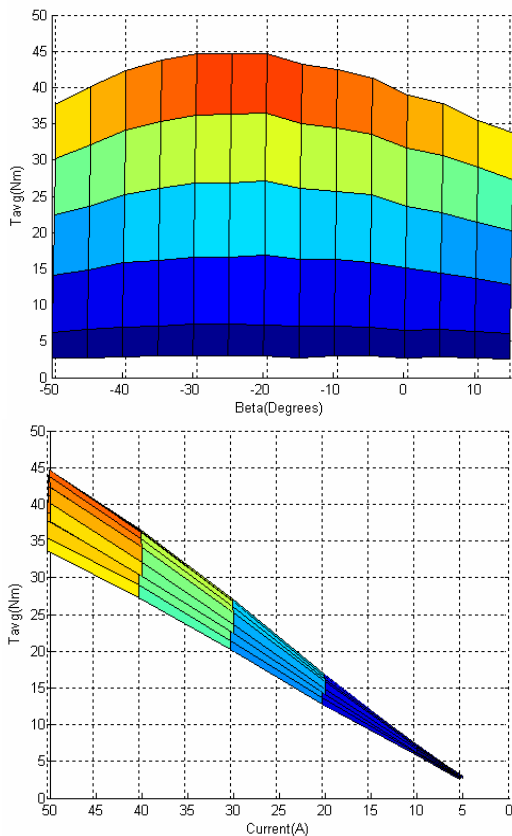


**Fig. 13.** 2-D curves for the  $T_{avg}$  of the Hybrid1: (a)  $T_{avg}$ - $\beta$  curve; (b)  $T_{avg}$ -Current curve

It is seen from Fig. 13 that the distribution of the colors shows the concentrated region for the  $T_{avg}$ . Examining the graphs by this method, it is seen that at low currents,  $\beta$  does not affect the  $T_{avg}$  and  $T_{max}$  values so much. However,  $\beta$  becomes a remarkable parameter by the increase of the current. The concentrated regions of the 3-D graphs for the hybrid motors were determined and acceptable  $\beta$  ranges

were obtained for  $T_{avgmax}$  and  $T_{max}$  values. Table 6 gives the  $\beta$  ranges for the hybrid motors.

**Table 6.** Acceptable  $\beta$  range for  $T_{avgmax}$  and  $T_{max}$  for the hybrid motors

Motor Type	$T_{avgmax}$ $\beta$ Range (Degrees)	$T_{max}$ $\beta$ Range (Degrees)
Hybrid1	-30° - -15°	-30° - -15°
Hybrid2	-30° - -10°	-30° - -15°
Hybrid3	-20° - 0°	-20° - 0°
Hybrid4	-20° - 0°	-20° - 0°
Hybrid5	-30° - 5°	-25° - 0°

Another considerable result can be seen from Table 3 that the Reluctance generates higher  $T_{avg}$  and  $T_{max}$  values than the Magnet by the increase of the current. Then, it is seen from Fig. 12 that when the ratio of the reluctance component increases in the hybrid rotors, the generated  $T_{avg}$  and  $T_{max}$  values increase.

### 5. Conclusion

A hybrid motor structure that is suitable to modify the rotor hybridization ratio was proposed in this paper. The paper briefly includes introducing the motor structure, FE analysis and experimental study of the proposed hybrid motor. The simulation and experimental results were compared and a detailed study was made for the experimental tests. The presentable results of the study are summarized as follows:

- (1) The hybridization ratio on the rotor is provided by the magnet and reluctance parts for the proposed hybrid motor. The magnet and reluctance parts consist of 6 pieces and the rotor can be assembled for

various hybridization ratios. Therefore the magnet and reluctance torques on the rotor can be modified by the proposed motor type.

- (2) Due to the toothed structure of the magnet and reluctance pieces and the rotor shaft, the position of the pieces can be rotated with respect to each other with 5 mechanical degrees.
- (3) The generated torque is the sum of the magnet and reluctance torques in the proposed motor. Due to the items (1) and (2), the total torque is affected by the ratio of the pieces and the mechanical angle ( $\beta$ ) between the parts.
- (4) Varying both the hybridization ratio and the angle  $\beta$  together, the generated torque profiles were first calculated by FE analysis for different current values. Then the static torque measurements were realized for the Magnet, the Reluctance and hybrid motor types. 14 different  $\beta$  values were used between the magnet and reluctance parts, and so 70 rotor types were examined for 5 hybrid rotor structure.
- (5)  $T_{avg}$  and  $T_{max}$  values were obtained from the calculated and measured torque profiles and considering the measurements 3-D graphs were formed to analyze the results related to current and  $\beta$ . It was seen that different combinations on the rotor showed different torque behavior.  $T_{avg}$  was calculated for electrical 120° operation mode,  $T_{max}$  was calculated to prepare the preliminary study for the vector control.
- (6) The simulated and experimental  $T_{avg}$  and  $T_{max}$  values were compared with each other for the specific current and  $\beta$  values. The results were similar. Thus, it can be said that FE simulations give considerable idea about the proposed motor types considering  $T_{avg}$  and  $T_{max}$  values.
- (7) Acceptable  $\beta$  ranges were obtained for  $T_{avgmax}$  and  $T_{max}$  values of the hybrid motor types. Each motor type has a specific region for  $T_{avgmax}$  and  $T_{max}$ .
- (8) The Magnet generates higher torque values at low currents. However the Reluctance shows higher performance considering the generated torque by the increase of the current. Then the Magnet resembles a permanent magnet dc motor and the Reluctance resembles a serial dc motor. So it can be said that because the proposed hybrid motor types consist of the magnet and reluctance parts, they show different compound dc motor characteristics.

These results show that changing the amount and position of the magnet and reluctance torques on the rotor provides different properties for the proposed motor. It is thought to benefit from the obtained data in this study and improve a control method for the proposed motor types for the future study.

## References

- [1] B. J. Chalmers, L. Musaba and D. F. Gosden, "Variable -Frequency Synchronous Motor Drives for Electrical Drives", *IEEE Transactions on Industry Applications*, vol. 32 no. 4, pp. 896-903, August 1996.
- [2] B. J. Chalmers, R. Akmesse and L. Musaba, "Design and Field Weakening Performance of Permanent-Magnet/Reluctance Motor with Two-Part Rotor", *IEE Proceedings-Electric Power Applications*, vol. 145, no. 2, 1998.
- [3] W. Guo, Z. Zhao and Y. Zhang, "Analysis and Experimental Study of Slot Effect in Synchronous Reluctance Permanent Magnet Motors", *5<sup>th</sup> International Power Electronics and Motion Control Conference ~IPEMC 2006~*, August 2006.
- [4] W. Guo and Z. Zhao, "Design and Experiments of Two Glued Axially Laminated Synchronous Reluctance Permanent Magnetic Motors", *International Conference on Power Electronics and Drive Systems ~PEDS 2005~*, 2005.
- [5] P. Niazi, H. A. Toliyat, D. H. Cheong and J. C. Kim, "A Low-Cost and Efficient Permanent-Magnet-Assisted Synchronous Reluctance Motor Drive", *IEEE Transactions on Industry Applications*, vol. 43 no. 2, pp. 542-550, 2007.
- [6] P. Niazi and H. A. Toliyat, "Design of a Low-Cost Concentric Winding Permanent Magnet Assisted Synchronous Reluctance Motor Drive", *IEEE 40<sup>th</sup> IAS Annual Meeting*, 2005.
- [7] S. Talebi, P. Niazi and H. A. Toliyat, "Design of a Permanent Magnet Assisted Synchronous Reluctance Motors Made Easy", *IEEE 42<sup>nd</sup> IAS Annual Meeting*, September 2007.
- [8] P. Guglielmi, G. Giraudo, G.M. Pellegrino and A. Vagati, "Pm Assisted Synchronous Reluctance Drive for Minimal Hybrid Application", *IEEE 39<sup>th</sup> IAS Annual Meeting*, October 2004.
- [9] N. Bianchi, S. Bolognani, D. Bon and M. Dai Pre, "Rotor Flux-Barrier Design for Torque Ripple Reduction in Synchronous Reluctance and Pm Assisted Synchronous Reluctance Motors", *IEEE Transactions on Industry Applications*, vol. 45 no. 3, pp. 921-928, May 2009.
- [10] C. L. Gu, B. J. Chalmers and C. W. Lu, "Rotor Design Optimization of a Synchronous Machine with Two Part Rotor", *IEEE International Electric Machines and Drives Conference*, 1997.
- [11] E. Kandemir Beser, S. Camur, B. Arifoglu and E. Beser, "Application of a Four-pole Hybrid Motor Structure Suitable for Modifying the Rotor Hybridization Ratio", *International Review of Electrical Engineering*, vol.5, no.5, pp. 2049-2056, September-October 2010.
- [12] W. L. Soong, D. A. Staton and T. J. E. Miller, "Design of a New Axially-Laminated Interior



Permanent Magnet Motor”, *IEEE Transactions on Industry Applications*, vol. 31 no. 2, pp. 358-367, May 1995.

- [13] I. Boldea and S. Nasar, “Emerging Electric Machines with Axially Laminated Anisotropic Rotors: a Review”, *Electrical Machines and Power Systems*, vol. 19, pp. 673-704, 1991.



**Esra Kandemir Beser** She was born in Kocaeli, Turkey, on June 10, 1980. She received the B.S. and M.S. degrees in electrical engineering from Kocaeli University, Kocaeli, Turkey, in 2002 and 2004, where she is currently working toward the Ph.D. degree. She has been a research assistant with the Department of Electrical Engineering, Kocaeli University since 2002. Her research interests include design and analysis of electrical machines, brushless dc motors and drives, motor control, power electronics and multilevel inverters.



**Sabri Camur** He was born in Adapazari, Turkey, on March 14, 1965. He received the B.S. and M.S. degrees in electrical engineering from Yildiz University, Istanbul, Turkey, in 1989 and 1991, respectively, and the Ph.D. degree from Kocaeli University, Kocaeli, Turkey, in 1998. Currently, he is an Assistant Professor with the Department of Electrical Engineering, Kocaeli University. His research interests are design and control of electrical machines, power electronics, multilevel inverters, reactive power compensation, solar energy and applications, electronics and industrial electronics.



**Birol Arifoglu** He was born in Ksanti, Greece, on June 5, 1968. He received the B.S. degree in electrical engineering from Yildiz University, Istanbul, Turkey, in 1989, the M.S. degree from Istanbul Technical University, Istanbul, Turkey, in 1993 and the Ph.D. degree from Kocaeli University, Kocaeli, Turkey, in 1998. Currently, he is an Assistant Professor with the Department of Electrical Engineering, Kocaeli University. His research interests are in the areas of power electronics, dc-dc converters, inverters, automatic control and applications, PLC and SCADA applications, wind energy and industrial electronics and applications.



**Ersoy Beser** He was born in Kocaeli, Turkey, on March 23, 1977. He received the B.S., M.S. and Ph.D. degrees in electrical engineering from Kocaeli University, Kocaeli, Turkey, in 2000, 2004 and 2009 respectively. Currently, he is an Assistant Professor with the Department of Electrical Engineering, Kocaeli University. His research interests are power electronics, multilevel inverters, electrical machines, motor control and microprocessors.